ELSEVIER

Ceramics International 30 (2004) 1725–1729

CERAMICS INTERNATIONAL

www.elsevier.com/locate/ceramint

Fabrication of zinc oxide nanostructures on gold-coated silicon substrate by thermal chemical reactions vapor transport deposition in air

B.J. Chen, X.W. Sun*, C.X. Xu

School of Electrical and Electronic Engineering, Nanyang Technological University, Nanyang Avenue, Singapore 639798, Singapore

Received 6 November 2003; received in revised form 2 December 2003; accepted 22 December 2003

Available online 6 May 2004

Abstract

Zinc oxide nanostructures (nanowires, nanobelts, and nanofibers) were fabricated on gold-coated silicon (1 0 0) substrate via a simple thermal chemical reactions vapor transport deposition (TCRVTD) method in air with a mixture of ZnO and carbon powders as reactants. The growth process was carried out at 1100 °C in a quartz tube with one side open to the air. The gold film acted as a metal catalyst. There is no carrier gas in the process. The ZnO nanostructures were characterized by the scanning electron microscope (SEM), X-ray diffraction (XRD), Raman spectroscopy, and room temperature photoluminescence (PL) spectroscopy. The growth mechanism is explained by thermal chemical reactions and vapor–liquid–solid growth mechanism.

Keywords: D. Zinc oxide; Nanostructure; Scanning electron microscope; Raman spectroscopy

Zinc oxide (ZnO) is a II–VI compound semiconductor with a wide direct energy bandgap of 3.37 eV, and a large excitonic binding energy of about 60 meV at room temperature. ZnO is promising for applications in blue light-emitting diodes (LEDs), field-effect transistors (FET), ultraviolet laser diodes (LD), sensors, acousto-electrical devices, and detectors. Nanostructural ZnO has attracted much more attention owing to their great potential for fundamental studies as well as for applications in one-dimensional nanodevices and other functional materials. In addition to nanotubes [1], nanowires [2] and nanorods [3], other interesting nanostructures such as nanoribbons [4], and nanobelts [5] have also been demonstrated recently. As the luminescence of ZnO is very sensitive to its surface states [6], ZnO nanostructures with a high surface to bulk ratio are expected to make possible novel practical applications for electro-optical devices and chemical sensors.

Good quality ZnO materials have been prepared by many methods, including sputtering [7], pulse laser deposition (PLD) [8–10], metal organic chemical vapor deposition (MOCVD) [11–14], reactive thermal and electron beam evaporation [15], spray pyrolysis [16], oxidation of metallic Zinc [17], ion beam assisted deposition [18], sol–gel [19], atomic layer deposition, molecular beam epitaxy [20,21]. In this paper, we report a simple thermal chemical reactions vapor transport deposition (TCRVTD) method for growth of ZnO nanocrystal structures on gold coated silicon substrate in air by sintering ZnO and carbon powders as reactants. The gold film acted as a catalyst in the reaction. There is no additional carrier gas in the process.

A horizontal one-side opened quartz tube (inner diameter: 50 mm, length: 100 cm) was placed inside a high-temperature tube furnace as shown in Fig. 1. The mixture of high purity ZnO (99.999%) and carbon powders (in molar ratio of 1:2) was loaded at the end of a slender one-end sealed quartz tube (inner diameter: 12 mm, length: 20 cm). A cleaned silicon wafer with (1 0 0) orientation was coated with a layer of gold using a vacuum thermal evaporator. The thickness of the gold films is about 200 Å measured by surface profilometer (Alpha-step, TENCOR P-10). The gold-coated silicon substrate was put into the small quartz tube as a collector. Then the small quartz

* Corresponding author. Tel.: +65-67905369; fax: +65-67933318.
E-mail address: exwsun@ntu.edu.sg (X.W. Sun).

0272-8842/$30.00
doi:10.1016/j.ceramint.2003.12.140

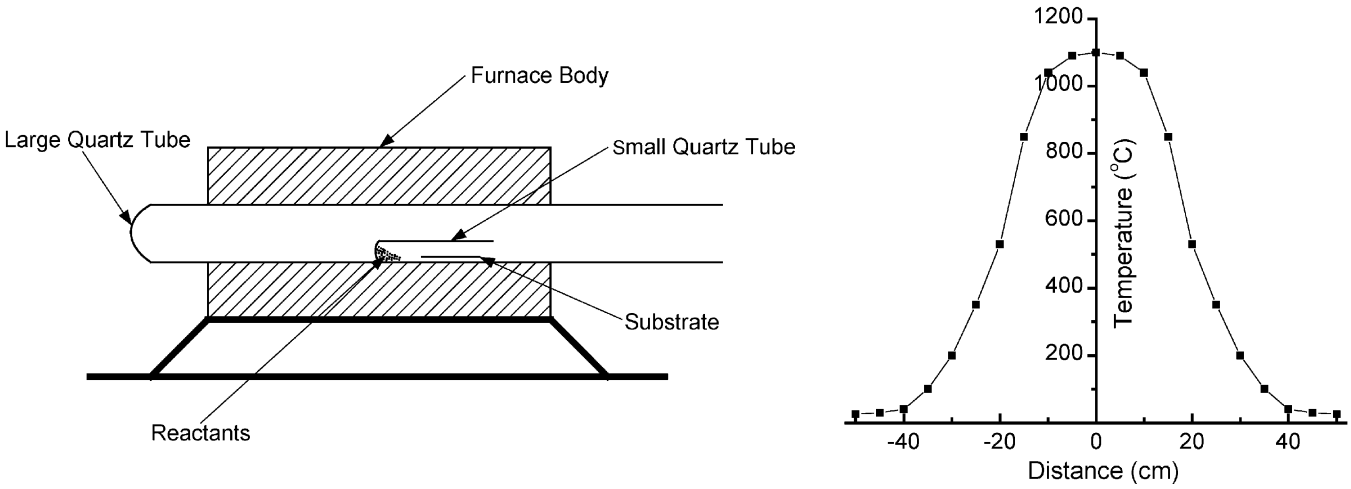

Fig. 1. ZnO nanostructure growth system and its temperature distribution.

tube with reactive source and silicon substrate was placed into the bigger quartz tube and pushed to the center of the furnace. The reactants were heated at 1100 °C. The temperature of the substrate region was a little lower than that of reactants due to the temperature gradient as shown in Fig. 1. After 30 min sintering, the small quartz tube was drawn out from the furnace and cooled down to the room temperature in air. White and grayish-white color products formed on the surface of the silicon substrate.

The morphology of the materials on the substrate was examined by a JEOL JSM-5910LV scanning electron microscope (SEM) at low and medium magnifications, respectively. Powder X-ray diffraction (XRD) patterns were obtained by a Siemens D-5005 diffractometer by using copper-monochromatized Cu Kα1 radiation (λ = 1.540598 Å) under the accelerating voltage of 40 kV and the current of 40 mA with a normal θ–2θ scan. Raman spectra of the sample were measured by using a Renishaw micro-Raman System 1000 spectrometer with excitation from an Ar^+ laser operating at 514.5 nm. Photoluminescence (PL) measurement was performed at room temperature using a Xenon lamp (250–2000 nm) operating at 325 nm as the excitation source.

Typical SEM images of the ZnO products grown on the gold-coated silicon substrate are shown in Fig. 2. Three kinds of morphologies, namely nanowires (Fig. 2a and b), nanobelts (Fig. 2c) and nanofibers (Fig. 2d) are shown, which dependent on the distance from the reactants or growth temperature. The region of nanowires is nearest, while the region of nanofibers is farthest to the reactants. The region of nanobelts is between that of nanowires and nanofibers on the substrate.

Fig. 2a shows the image of ZnO nanowires formed in low density near the edge of the substrate. In most area of the substrate, the flexural and uniform ZnO nanowires were formed in very high yield as shown in Fig. 2b. The diameters of nanowires normally range from 40 to 80 nm and their lengths are about 40–120 μm on the surface of the sample, but most nanowires are entangled with one another (Fig. 2b) that makes it hard to measure the length accurately. Fig. 2c shows the morphology of ZnO nanobelts region. The belts look like grain leaves, there are some nanowires can be seen among the belts. The morphology of the ZnO nanofibers is shown in Fig. 3a. It can be seen that the obtained ZnO fibers with uniform diameters 160 nm and the length up to 40 μm, which resulting in aspect ratio estimated as high as about 250.

Fig. 3 shows the XRD pattern of the deposited products on the gold-coated silicon substrate. All the diffraction peaks in the figure can be indexed to the known hexagonal wurtzite structure of ZnO with cell parameters of $a = b = 3.242$ Å, and $c = 5.205$ Å. The strong intensity and narrow width of ZnO diffraction peaks indicate that the resulting products were of high crystallinity. Gold (1 1 1) peaks have also be detected in our samples. The peak at about 57.9° is attributed to the silicon oxide for the nanobelts and nanofibers samples.

Raman scattering measurement of the ZnO products was performed at room temperature. The spectra are shown in Fig. 4. In Fig. 4, the peaks at 437 and 1120 cm^{-1} are due to high frequency vibration modes of E_2 and $2E_1$ (LO) [22], respectively. The E_2 mode corresponds to band characteristic of wurtzite phase, the appearance of the $2E_1$ (LO) peak is attributed to the formation of oxygen vacancy, zinc interstitial defect states, and free carriers. Strong coupling of free carrier with E_1 (LO) mode would cause broadening of the line-width, frequency down shift, and asymmetric line-shape. The peak at 332 cm^{-1} is the second-order Raman spectrum arising from zone-boundary phonons $2E_2$ (M) [23]. The nanofibers show the second order Raman shift peak at about 1120 cm^{-1} with strongest intensity and narrowest line-width. Among of these Raman shift peaks, the E_2 mode peak at 437 cm^{-1} has the stronger intensity and narrower line-width, which indicate that the nanostructures are composed of ZnO with hexagonal wurtzite structure and good crystal quality.

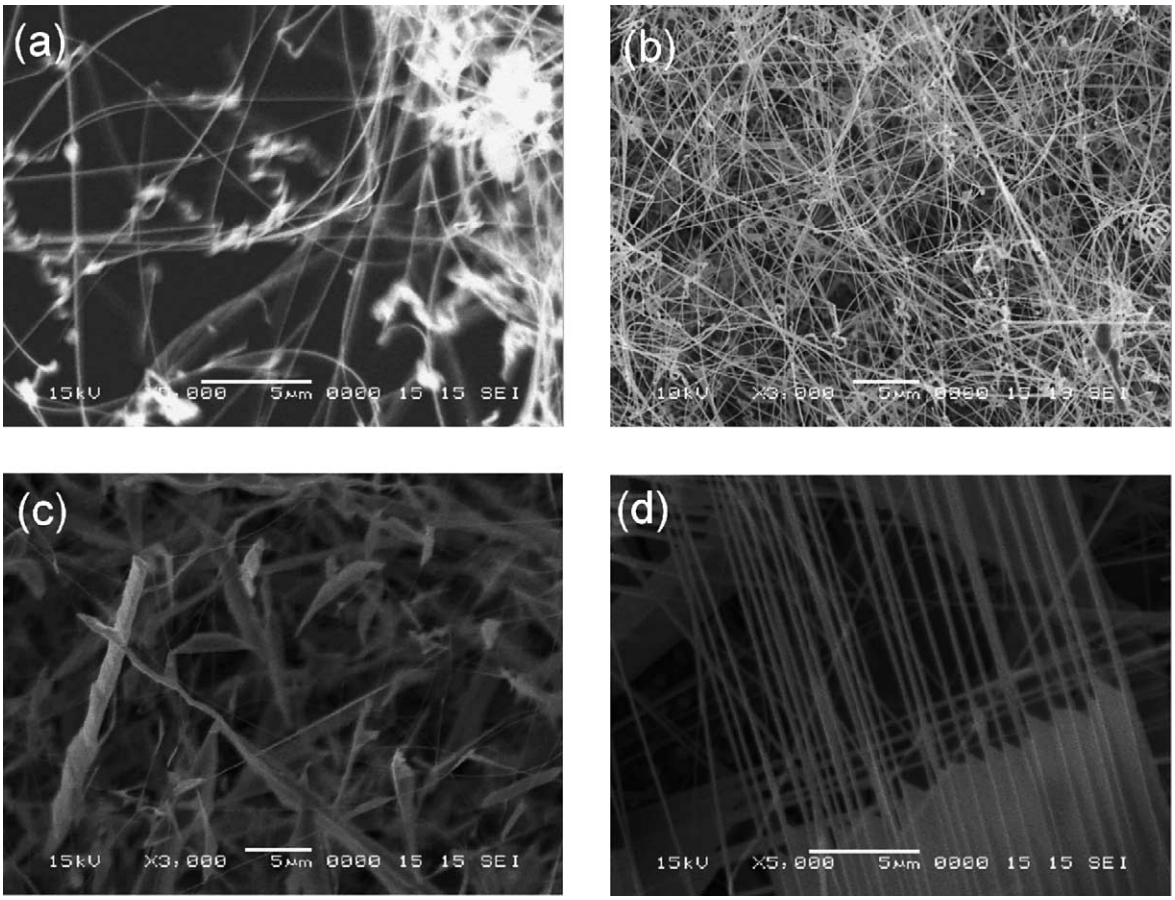

Fig. 2. SEM images of the ZnO nanostructures formed on gold-coated silicon substrate: (a) nanowires in low density region, (b) nanowires in high density region, (c) nanobelts, and (d) nanofibers.

The optical properties of the ZnO nanostructurers were characterized by the PL spectrum measurement at room temperature. As shown in Fig. 5, besides the UV band at 395 nm and a green band at about 500 nm, there is also a broad blue band with a few peaks at 438, 451, 463, 469, 474, and 481 nm. The UV emission band is due to a near-band edge (NBE) transition of wide band gap of ZnO, namely the recombination of free excitons through an exciton–exciton collision process. The green band emission is attributed to the radial recombination of a photo-generated hole with electron that belongs to the singly ionized oxygen vacancy in the surface and sub-surface lattices of ZnO materials. The blue bands may originate from impurity dopants, such as gold, in the growth of ZnO nanostructures. The ZnO nanowires exhibited strongest UV emission compared to the green band, while the ZnO nanofibes exhibited weakest PL emission from UV to green band. The PL trend correlates well with the crystal quality (Fig. 3) and the growth temperature.

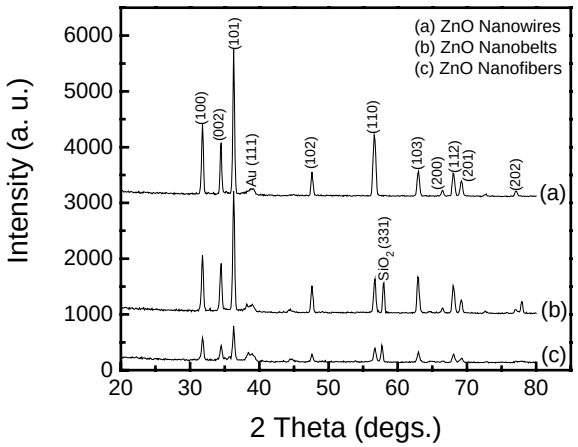

Fig. 3. XRD pattern of the ZnO nanostructures formed on gold-coated silicon substrate: (a) nanowires in low density region, (b) nanowires in high density region, (c) nanobelts, and (d) nanofibers.

The influence of sintering temperature (source temperature) and time on the formation of ZnO nanocrystal materials were also investigated. There was no ZnO products formed at sintering temperatures below 900 °C, while the products tend to form ZnO powders at sintering temperature of 1200 °C. It was found that the optimum sintering temperature for the present experiment of ZnO nanostructures was about 1100 °C. At growth temperature of 1100 °C, the growth rates and the resultant yield were mainly influenced by the quantity of the carbon powders. ZnO products could not be obtained by heating ZnO powders without carbon

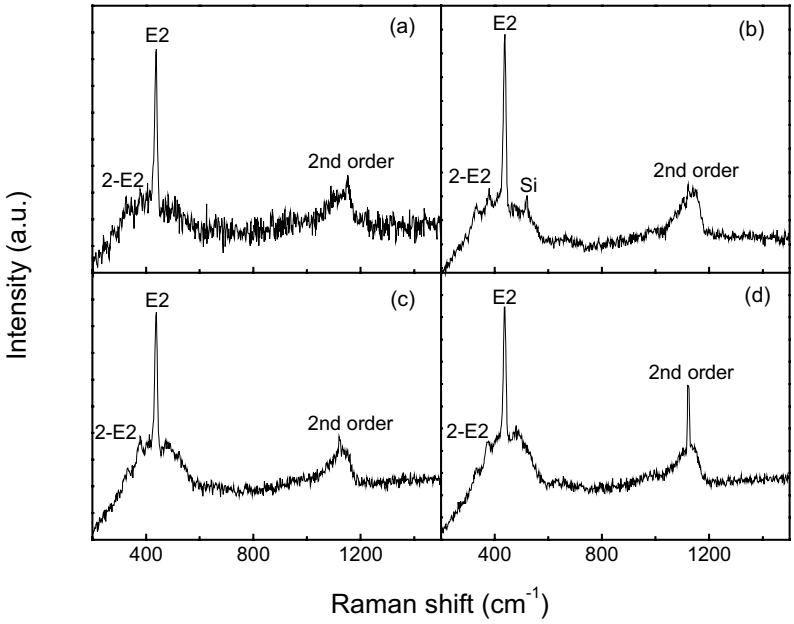

Fig. 4. Raman spectra of ZnO nanostructures formed on gold-coated silicon substrate: (a) low density nanowires, (b) high density nanowires, (c) nanobelts, and (d) nanofibers.

powders at our experiment conditions due to the high melting point of ZnO (1975 °C). Fewer ZnO products were obtained when a small quantity of carbon powders were mixed with ZnO powders as reactants, when excess carbon powders were added into the reactants, the growth rates became faster and the wires were longer. Carbon powders and its reaction resultants with oxygen, carbon oxide (CO), acted as reduction agents during ZnO formation. ZnO powders were reduced into Zn or its sub-oxide (ZnO_x, $x < 1$) with low melting point (~419 °C), they should be in vapor phase at the present experimental temperature. The Zn and ZnO_x transfered to the low temperature region and recombined with oxygen again to form ZnO products. At the low temperature region (lower than the boiling point of Zn, 907 °C), Zn or ZnO_x vapor became liquid droplets first, then reacted with the gold catalyst on the silicon substrate to form alloy droplets, which acted as nuclei of ZnO nanocrystal structure. The vapor pressure of Zn, ZnO_x, and CO was gradually decreased from the powder source to the open side of the quartz tube. The CO vapor suppressed ZnO formation due to its reduction effect at the high-temperature region of the substrate. At the other end of substrate far from the source, the vapor of Zn and ZnO_x was too low to grow ZnO. This vapor–liquid–solid (VLS) growth mechanism was also proved by another experiment phenomenon. A uniform metal-like thin film with light-black color was deposited on the wall of the large quartz tube near the open end of the tube when the same quantity mixture was heated at the temperature of 1100 °C by pumping the large quartz tube to a vacuum of about 2 T. This indicated that Zn and ZnO_x reduced from ZnO did not reform ZnO due to lack of oxygen under the low vacuum.

ZnO nanostructures were grown by using ZnO and carbon powders as reactants on the gold-coated silicon substrate through a simple thermal reaction vapor transport method in air. The obtained ZnO nanowires had diameters ranging from ranging from 40 to 80 nm and the maximal lengths up to 120 μm on the surface of the substrate. The ZnO fibers had uniform diameters of 160 nm and the length up to 40 μm, which resulting in an aspect ratio estimated as high as about 250. XRD and Raman spectra showed that the nanostructures were composed of hexagonal wurtzite-phase ZnO with good crystal quality. The good crystallinity of the ZnO fibers had also been verfied by room temperature PL spectra with the narrow UV band at 395 nm and a broad green band at about

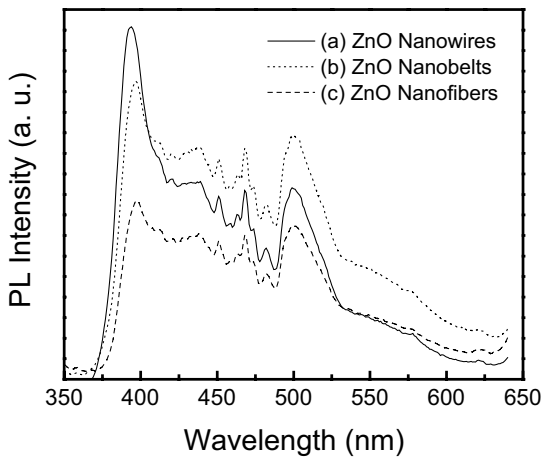

Fig. 5. PL spectra of ZnO nanostructures on gold-coated silicon substrate: (a) nanowires, (b) nanobelts, and (c) nanofibers.

500 nm. The growth mechanism was explained by chemical reactions and vapor–liquid–solid (VLS) deposition process with gold as catalyst.

References

[1] J.-J. Wu, S.-C. Liu, C.-T. Wu, K.-h. Chen, L.-C. Chen, Heterostructures of ZnO–Zn coaxial nanocables and ZnO nanotubes, Appl. Phys. Lett. 81 (7) (2002) 1312–1314.

[2] M.H. Huang, Y. Wu, H. Feick, N. Tran, E. Weber, P. Yang, Catalytic growth of zinc oxide nanowires by vapor transport, Adv. Mater. 13 (2) (2001) 113–116.

[3] Y.W. Heo, V. Varadarajan, M. Kaufman, K. Kim, D.P. Norton, F. Ren, P.H. Fleming, Site-spectific growth of ZnO nanorods using catalysis-driven molecular-beam epitaxy, Appl. Phys. Lett. 81 (16) (2002) 3046–3048.

[4] B.D. Yao, Y.F. Chan, N. Wang, Formation of ZnO nanostructures by a simple way of thermal evaporation, Appl. Phys. Lett. 81 (4) (2002) 757–759.

[5] Y.B. Li, Y. Bando, T. Sato, K. Kurashima, ZnO nanobelts grown on Si substrate, Appl. Phys. Lett. 81 (1) (2002) 144–146.

[6] B.D. Yao, H.Z. Shi, H.J. Bi, L.D. Zhang, Optical properties of ZnO loaded in mesoporous silica, J. Phys.: Condens. Mater. 12 (28) (2000) 6265–6270.

[7] K.K. Kim, J.H. Song, H.J. Jung, S.J. Park, The grain size effects on the photoluminescence of ZnO/α-Al_2O_3 grown by radio-frequency magnetron sputtering, J. Appl. Phys. 87 (7) (2000) 3573–3575.

[8] Y.R. Ryu, S. Zhu, J.D. Budai, H.R. Chandrasekhar, P.F. Miceli, H.W. White, Optical and structural properties of ZnO films deposited on GaAs by pulsed laser deposition, J. Appl. Phys. 88 (1) (2000) 201–204.

[9] B.J. Jin, S. Im, S.Y. Lee, Violet and UV luminescence emitted from ZnO thin films grown on sapphire by pulsed laser deposition, Thin Solid Films 366 (1/2) (2000) 107–110.

[10] X.W. Sun, H.S. Kwok, Optical properties of epitaxially grown zinc oxide films on sapphire by pulsed laser deposition, J. Appl. Phys. 86 (1) (1999) 408–411.

[11] F.T.J. Smith, Metalorganic chemical vapor deposition of oriented ZnO films over large areas, Appl. Phys. Lett. 43 (12) (1983) 1108–1110.

[12] K. Haga, F. Katahira, H. Watanabe, Preparation of ZnO films by atmospheric pressure chemical-vapor deposition using zinc acetylacetonate and ozone, Thin Solid Films 343–344 (1999) 145–147.

[13] K. Ogata, T. Kawanishi, K. Maejima, K. Sakurai, S. Fujita, S. Fujita, Improvements of ZnO qualities grown by metal-organic vapor phase epitaxy using a molecular beam epitaxy grown ZnO layer as a substrate, Jpn. J. Appl. Phys. Part 2 40 (7A) (2001) L657–L659.

[14] S. Suh, D.M. Hoffman, L.M. Atagi, D.C. Smith, A new metal-organic precursor for the low-temperature atmospheric pressure chemical vapor deposition of zinc oxide films, J. Mater. Sci. Lett. 18 (10) (1999) 789–791.

[15] H.Z. Wu, K.M. He, D.J. Qui, D.M. Huang, Low-temperature epitaxy of ZnO films on Si(0 0 1) and silica by reactive e-beam evaporation, J. Cryst. Growth 217 (1/2) (2000) 131–137.

[16] S.A. Studenikin, N. Golego, M. Cocivera, Fabrication of green and orange photoluminescent, undoped ZnO films using spray pyrolysis, J. Appl. Phys. 84 (4) (1998) 2287–2294.

[17] S.L. Cho, J. Ma, Y.K. Kim, Y. Sun, G.K.L. Wong, J.B. Ketterson, Photoluminescence and ultraviolet lasing of polycrystalline ZnO thin films prepared by the oxidation of the metallic Zn, Appl. Phys. Lett. 75 (18) (1999) 2761–2763.

[18] W. Li, D.S. Mao, Z.H. Zheng, X. Wang, X.H. Liu, S.C. Zou, Y.K. Zhu, Q. Li, J.F. Xu, ZnO/Zn phosphor thin films prepared by IBED, Surf. Coat. Technol. 128/129 (2000) 346–350.

[19] T. Nagase, T. Ooie, Y. Nakatsuka, K. Shinozaki, N. Mizutani, A novel method for the preparation of green photoluminescent undoped zinc oxide film involving excimer laser irradiation of a sol–gel-derived precursor, Jpn. J. Appl. Phys. Part 2 39 (7B) (2000) L713–L715.

[20] Y.F. Chen, D. Bagnall, T.F. Yao, ZnO as a novel photonic material for the UV region, Mater. Sci. Eng. B 75 (2/3) (2000) 190–198.

[21] T. Makino, G. Isoya, Y. Segawa, C.H. Chia, T. Yasuda, M. Kawasaki, A. Ohtomo, K. Tamura, H. Koinuma, Optical spectra in ZnO thin films on lattice-matched substrates grown with laser-MBE method, J. Cryst. Growth 214/215 (2000) 289–293.

[22] J.N. Zeng, J.K. Low, Z.M. Ren, T. Liew, Y.F. Lu, Effect of deposition conditions on optical and electrical properties of ZnO films prepared by pulsed laser deposition, Appl. Surf. Sci. 197/198 (2002) 362–367.

[23] J.M. Calleja, M. Cardona, Resonant Raman scattering in ZnO, Phys. Rev. B 16 (8) (1977) 3753–3761.